



Water/Ethanol and 13X Zeolite Pairs for Long-Term Thermal Energy Storage at Ambient Pressure

Matteo Fasano, Luca Bergamasco, Alessio Lombardo, Manuele Zanini, Eliodoro Chiavazzo and Pietro Asinari*

Department of Energy, Politecnico di Torino, Turin, Italy

OPEN ACCESS

Edited by:

A.E. Kabeel,
Tanta University, Egypt

Reviewed by:

Prasad Chandran,
Hindustan University, India
Yiji Lu,
Zhejiang University, China

*Correspondence:

Pietro Asinari
pietro.asinari@polito.it

Specialty section:

This article was submitted to
Solar Energy,
a section of the journal
Frontiers in Energy Research

Received: 23 April 2019

Accepted: 02 December 2019

Published: 18 December 2019

Citation:

Fasano M, Bergamasco L, Lombardo A, Zanini M, Chiavazzo E and Asinari P (2019) Water/Ethanol and 13X Zeolite Pairs for Long-Term Thermal Energy Storage at Ambient Pressure. *Front. Energy Res.* 7:148. doi: 10.3389/fenrg.2019.00148

Thermal energy storage is a key technology to increase the global energy share of renewables—by matching energy availability and demand—and to improve the fuel economy of energy systems—by recovery and reutilization of waste heat. In particular, the negligible heat losses of sorption technologies during the storing period make them ideal for applications where long-term storage is required. Current technologies are typically based on the sorption of vapor sorbates on solid sorbents, requiring cumbersome reactors and components operating at below ambient pressure. In this work, we report the experimental characterization of working pairs made of various liquid sorbates (distilled water, ethanol and their mixture) and a 13X zeolite sorbent at ambient pressure. The sorbent hydration by liquid sorbates shows lower heat storage performance than vapor hydration; yet, it provides similar heat storage density to that obtainable by latent heat storage (40–50 kWh/m³) at comparable costs, robustness and simplicity of the system, while gaining the long-term storage capabilities of sorption-based technologies. As a representative application example of long-term storage, we verify the feasibility of a sorption heat storage system with liquid sorbate, which could be used to improve the cold-start of stand-by generators driven by internal combustion engines. This example shows that liquid hydration may be adopted as a simple and low-cost alternative to more efficient—yet more expensive—techniques for long-term energy storage.

Keywords: thermal energy storage, adsorption, zeolite, water, ethanol, experimental characterization

1. INTRODUCTION

Thermal Energy Storage (TES) systems allow to store excess thermal energy and to use it at a later time (Zhang et al., 2016). TES has recently attracted particular attention in the renewable energy field, to match periodical or intermittent availability of renewable sources (e.g., solar) with continuous energy demand (Díaz-González et al., 2012; Engel et al., 2017; Bocca et al., 2018). In this field, the design of efficient, reliable and economically-sustainable systems for thermal energy storage represents a major technological challenge to increase the renewable share on the global energy production (Ginley and Parilla, 2013). Thermal energy storage also finds application in the transport sector, for which a reduction of greenhouse gas emissions is foreseen by the recent international agreements on climate change mitigation (Schleussner et al., 2016; Xue et al., 2016). In general, TES techniques are mainly divided into three types: sensible, latent and thermo-chemical heat storage (Cabeza, 2015; Guo and Goumba, 2018).

Sensible heat storage is the most common and simple method, and relies on the capacity of a storage medium—e.g., solid or liquid—to store thermal energy by changing temperature. Clearly, large heat capacity is desirable to achieve high sensible heat storage density, namely the amount of stored energy in a given system per unit volume (Chidambaram et al., 2011). The thermal conductivity of the sensible heat storage material, instead, determines the duration of charging and discharging cycles (Cabeza et al., 2015). Typically, materials such as rock, concrete, steel, thermal oil and water are used for sensible heat storage (Hoogendoorn and Bart, 1992). Water has the advantages of having large specific heat capacity and lower cost with respect to other materials (IEA-ETSAP and IRENA, 2013); however, relatively low values in thermal conductivity lead to slower thermal responses (Ouden, 1981). Sensible heat storage finds application in domestic systems, district heating, industrial plants (Alva et al., 2018), solar (Andreozzi et al., 2012) and automotive systems (Ap and Golm, 1995; Aguiar et al., 2013). However, the low heat storage density of sensible heat storage—which is typically in the range 0–70 kWh/m³ (Lizana et al., 2017)—represents a severe bottleneck in applications with limited free volume available, e.g., in case of automobiles.

Latent heat storage relies on phase-change materials (PCMs), which accumulate latent heat via phase change—either from solid to liquid or from liquid to gas and vice-versa. Heat is stored in a narrow temperature range; therefore, PCM must have phase-transition temperature in the range of practical interest, besides being chemically stable, non-toxic and non-corrosive (Farid et al., 2004). Latent heat storage shows typically larger energy density than sensible one (about 30–100 kWh/m³, Lizana et al., 2017) and, thus, has been widely explored in solar (Andreozzi et al., 2018; Buonomo et al., 2018) and automotive applications (Jaguemont et al., 2018). The latter applications span from battery thermal management (Zhao et al., 2017) to engine pre-heating at start-up (Vasiliev et al., 1999; Gritsuk et al., 2016), from temperature optimization of engine for fuel saving (Kauranen et al., 2010; Shukla et al., 2017) to vehicle climate conditioning (Fleming et al., 2013; Jha and Badathala, 2015; Wang et al., 2017). However, both sensible and latent heat storage are prone to progressive degradation of the stored energy, which is due to thermal losses toward the surrounding environment and makes them unsuitable for long-term heat storage (Farid et al., 2004).

Thermo-chemical heat storage, instead, relies on reversible physical-chemical phenomena between compounds—namely the *working pair*—for energy accumulation or release via endothermic or exothermic reactions, respectively. Since heat is stored in the form of chemical potential and thermal losses are intrinsically minimal, thermo-chemical heat storage is suitable for long-term heat storage (N^oTsoukpoé et al., 2009). Besides chemical reactions (Donkers et al., 2016), thermo-chemical storage can be based also on sorption processes. This latter technique relies on the capacity of a sorbent material to take up a sorbate in the vapor or liquid phase. The sorption process may occur according to two different phenomena: absorption, if

the structure of the sorbent is modified by the sorbate sorption; adsorption, if the sorbate does not modify its structure during the process (N^oTsoukpoé et al., 2009). Based on the physical-chemical properties of the sorbent and sorbate, adsorption can be in turn classified as: physical adsorption (physisorption), mainly due to van der Waals forces; chemical adsorption (chemisorption), which results from chemical bond formation (McNaught and McNaught, 1997; Yu et al., 2013). While chemical reactions allow to achieve the highest energy densities (about 150–400 kWh/m³ Lizana et al., 2017) but also require large reaction temperatures, sorption processes generally provide a good compromise between high heat storage density (about 50–300 kWh/m³ Lizana et al., 2017), moderate reaction temperatures and cyclability (Cot-Gores et al., 2012).

Hence, heat storage systems based on sorption processes present the advantage of having: a large range of operating temperatures, depending on the chosen working pair; a larger heat storage density with respect to sensible and latent heat storage; negligible heat losses during the storing period, which makes them particularly suitable for long-term energy storage (Stritih and Bombač, 2014). Owing to these peculiar properties, and to the large range of potential applications, several working pairs have been extensively investigated: for example, sorbents like silica gel, zeolite, metal-organic framework or hygroscopic salts; sorbates as water or organic solvents (Scapino et al., 2017). A few works have also studied possible solar (Gaeini et al., 2018; Shere et al., 2018) or automotive (Gardie and Goetz, 1995; Narayanan et al., 2017) applications of TES based on sorption processes; however, a broader diffusion of this heat storage approach may be limited by the complexity of the required technology and auxiliary systems. In fact, since vapor-solid sorption is preferred to achieve larger heat storage density and improved adsorption/desorption dynamics, sorption heat storage systems typically require de-pressurized reactor vessels, vacuum pumps and various valves and tubes for managing the sorbate flow from/to the sorbent bed (Zettl et al., 2014). Such technological complexity does not represent an issue for building installations (e.g., heat pumps and seasonal TES, Calabrese et al., 2017; Vasta et al., 2018); whereas, this may be unpractical in applications where the simplicity of a long-term TES system should be prioritized with respect to its heat storage performance.

In this work, we characterize the heat storage potential of various liquid sorbates (distilled water, ethanol and a mixture thereof) on a commercial 13X zeolite sorbent at ambient pressure. Since no vacuum systems are needed to handle the liquid sorbents, this solution may be particularly suitable for robust, long-term, low-cost and electricity-free thermal energy storage systems. The considered sorbent material and the sorbate fluids are first presented, together with a detailed explanation of the experimental tests and instruments, in section 2. The experimental results are then reported in section 3, where the properties of different sorbent-sorbate pairs are compared. In section 4, the obtained results are used to outline an application example of the studied working pairs for long-term heat storage. Conclusions are finally drawn in section 5.

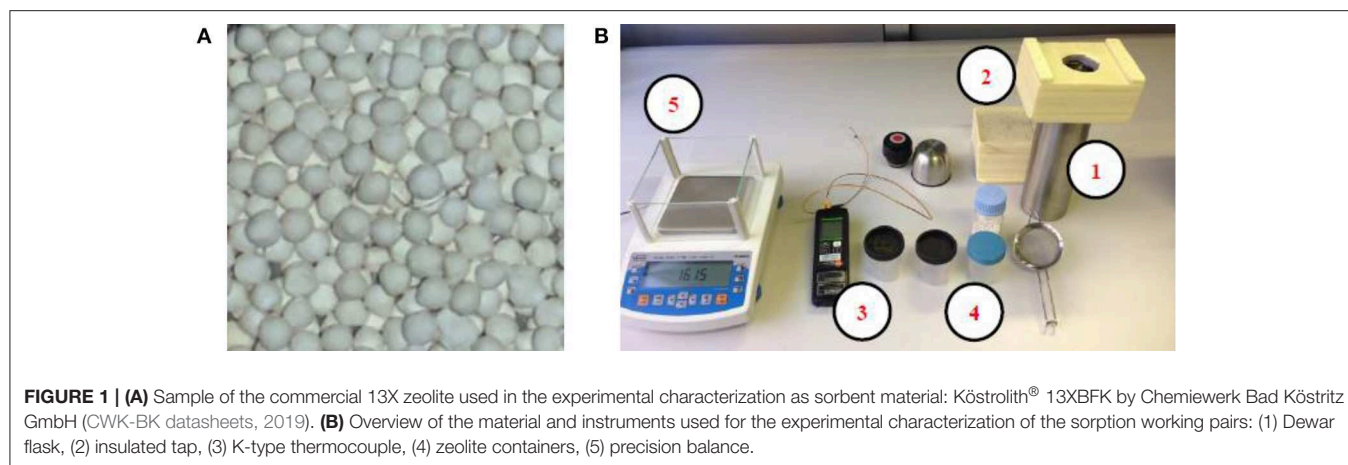


FIGURE 1 | (A) Sample of the commercial 13X zeolite used in the experimental characterization as sorbent material: Köstrolith® 13XBFK by Chemiewerk Bad Köstritz GmbH (CWK-BK datasheets, 2019). **(B)** Overview of the material and instruments used for the experimental characterization of the sorption working pairs: (1) Dewar flask, (2) insulated tap, (3) K-type thermocouple, (4) zeolite containers, (5) precision balance.

2. MATERIALS AND METHODS

2.1. Working Pairs

The tested sorbent material is the Köstrolith® 13XBFK, that is, a synthetic crystalline aluminosilicate (zeolite) by Chemiewerk Bad Köstritz GmbH (CWK-BK datasheets, 2019). The material is non-toxic, low-cost (about 1 € per liter) and particularly suitable for adsorption processes, since no inert binder components are included (Gaeni et al., 2018). This synthetic zeolite belongs to the Faujasite (FAU) family (Baerlocher et al., 2007; First et al., 2011) and presents a regular nanoporous structure with mean pore size equal to 9 Å (Fasano et al., 2016a, 2017), which makes it suitable for sorption of small molecules such as water or organic solvents (Fasano et al., 2016b; Bergamasco et al., 2019). The zeolite samples are supplied as spherical beads with diameter in the range 2.5–3.5 mm (see Figure 1A).

Distilled water, ethanol (99.8%, Sigma-Aldrich®) and a mixture thereof (30% ethanol, 70% water by weight) have been considered as sorbates. The proportion between ethanol and water in the mixture has been chosen to achieve a good compromise between higher heat storage density and lower freezing temperature. In general, thermo-chemical heat storage relies on the sorbent hydration by sorbate vapor to achieve larger heat storage density. In this work, we aim at characterizing the feasibility of a sorption TES cycle with liquid sorbates at ambient conditions, thus not requiring auxiliary systems for vapor generation. While distilled water-zeolite is one of the most common working pairs for sorption heat storage (Miró et al., 2016), here—considering potential outdoor applications—fluids with lower freezing point have been also tested. In this sense, some preliminary tests using water-ethylene glycol mixtures led us to exclude their utilization, as they carbonize at 150°C therefore clogging and wasting the zeolite during the dehydration phase. Ethanol, instead, has not shown significant detrimental effects on the zeolite beads. Note that, at ambient pressure, the freezing points of pure ethanol and 30:70wt. ethanol-water mixture are approximately -114°C and -20°C , respectively (Flick, 1998).

2.2. Experimental Methods

Three laboratory tests are set up to characterize the zeolite properties for heat storage, namely: liquid sorbate hydration, dehydration and heat storage density. All tests are carried out for the three considered fluids, that is, water, ethanol and their mixture.

First, the performed hydration tests aim at characterizing the maximum sorbate uptake by the sorbent material, at ambient pressure ($p = 1$ bar) and temperature ($T = 20^{\circ}\text{C}$). During the hydration test, the dry zeolite beads (10 g per test) are placed in a container, which is then completely filled by the considered sorbate. Such excess of sorbate guarantees that the sorbent material achieves full hydration at the considered ambient conditions. The excess sorbate is successively removed from the container; whereas, the loaded mass of sorbate is estimated as the difference in weight between the zeolite beads before and after full hydration, using the precision balance shown in Figure 1B (Radwag® PS 1000_R2, 0.001 g resolution). At fully hydrated conditions, the fraction between the mass of loaded liquid ($m_{liq, fh}$) and the one of dry sorbent (m_{zeo}) is here defined as

$$\phi = \frac{m_{liq, fh}}{m_{zeo}}. \quad (1)$$

To assess the possible degradation of sorbents after multiple hydration/dehydration cycles, the hydrated zeolite beads are then dried in an oven with controlled temperature, and the hydration test repeated.

Second, dehydration tests are performed to measure the amount of sorbate released from the zeolite beads at different temperatures. Dry zeolite beads (10 g per test) are first fully hydrated according to the previously described protocol, and then introduced in an oven with controlled temperature and ambient pressure. These regeneration experiments are continued until two successive measures of R_g differ less than 5% between each other. The weight of the zeolite sample is monitored at different time intervals, thus obtaining the sorbate release rate with time. Here, the regeneration of the zeolite is intended as the dehydration process, which restores the heat storage

potential of the sorbent material, and it is quantified by the following parameter:

$$R_g = 1 - \frac{m_{liq}}{m_{liq, fh}} \tag{2}$$

where the mass of loaded liquid (m_{liq}) is compared with that in case of fully hydrated conditions ($m_{liq, fh}$) at ambient pressure. R_g is measured as a function of different regeneration temperatures and for the different tested sorbates.

Finally, the heat storage density (E_ρ) of the tested working pair is computed as

$$E_\rho = \frac{Q_r}{V_{zeo}} \tag{3}$$

being Q_r the thermal energy released in the hydration process and V_{zeo} the volume of dry zeolite. Q_r is obtained via calorimetric measurements, while $V_{zeo} = m_{zeo}/\rho_{zeo}$ with $\rho_{zeo} = 800 \text{ kg/m}^3$. A dewar flask has been employed for the calorimetric tests [see (1) in **Figure 1B**]. An adiabatic cap [see (2) in **Figure 1B**] has been designed to allow the insertion of zeolite beads into the dewar flask while minimizing thermal losses. The experiments are performed according to the following protocol. The zeolite beads (10 g per test) are first placed into the adiabatic cap; the liquid sorbate is poured into the flask. Note that an excess quantity of sorbate is introduced into the flask with respect to the actual $m_{liq, fh}$ (approximately 20% more, $k_{liq} = 1.2$), to ensure that the sorbent material achieves complete hydration. One thermocouple [K-type, RS Pro, Alberghini et al., 2019, see (3) in **Figure 1B**] is located inside the dewar flask, being initially immersed in the liquid sorbate. The cap is then positioned on the top of the flask, with a thin paper sheet preventing the zeolite beads from falling into the flask. The assembled measurement system is left to relax to ambient temperature. When thermal equilibrium is reached, the paper sheet is removed from the cap and the zeolite released into the flask. The sorbent reacts with the liquid sorbate, producing an exothermic reaction that releases heat (hydration process). Since the capped flask has negligible heat losses with the surrounding environment (less than 5%), the system can be reasonably approximated as adiabatic. Therefore, the thermal energy released by the hydration process can be estimated as:

$$Q_r = m_{zeo} c_{p, zeo} (T_e - T_i) + m_{liq, t} \int_{T_i}^{T_e} c_{p, liq}(T) dT \tag{4}$$

being T_i the initial temperature measured by the thermocouple inside the flask (before the hydration process), T_e the equilibrium temperature (when the hydration is complete), $m_{liq, t} = k_{liq} m_{liq, fh}$ is the total mass of the liquid sorbate, $c_{p, zeo}$ and $c_{p, liq}$ the specific heat capacity of the sorbent and sorbate, respectively. For the considered tests, the hydration process typically completes in less than 10 s.

3. RESULTS

3.1. Hydration Process

The experimental values of sorbate loaded in zeolite are shown in **Figure 2** for the three tested liquids, at $p = 1$ bar and $T = 20^\circ\text{C}$.

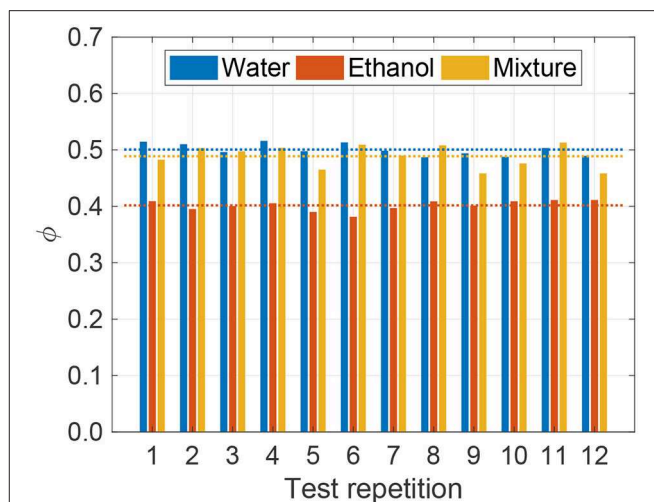


FIGURE 2 | Loaded liquid fraction (ϕ in Equation 1) obtained for twelve repetitions of the experimental characterization test at ambient pressure ($p = 1$ bar) and temperature ($T = 20^\circ\text{C}$) on pristine zeolite samples for the different tested fluids (water, ethanol and 30:70%wt. ethanol-water mixture). The dotted lines show the mean value over the repetitions for the three different fluids.

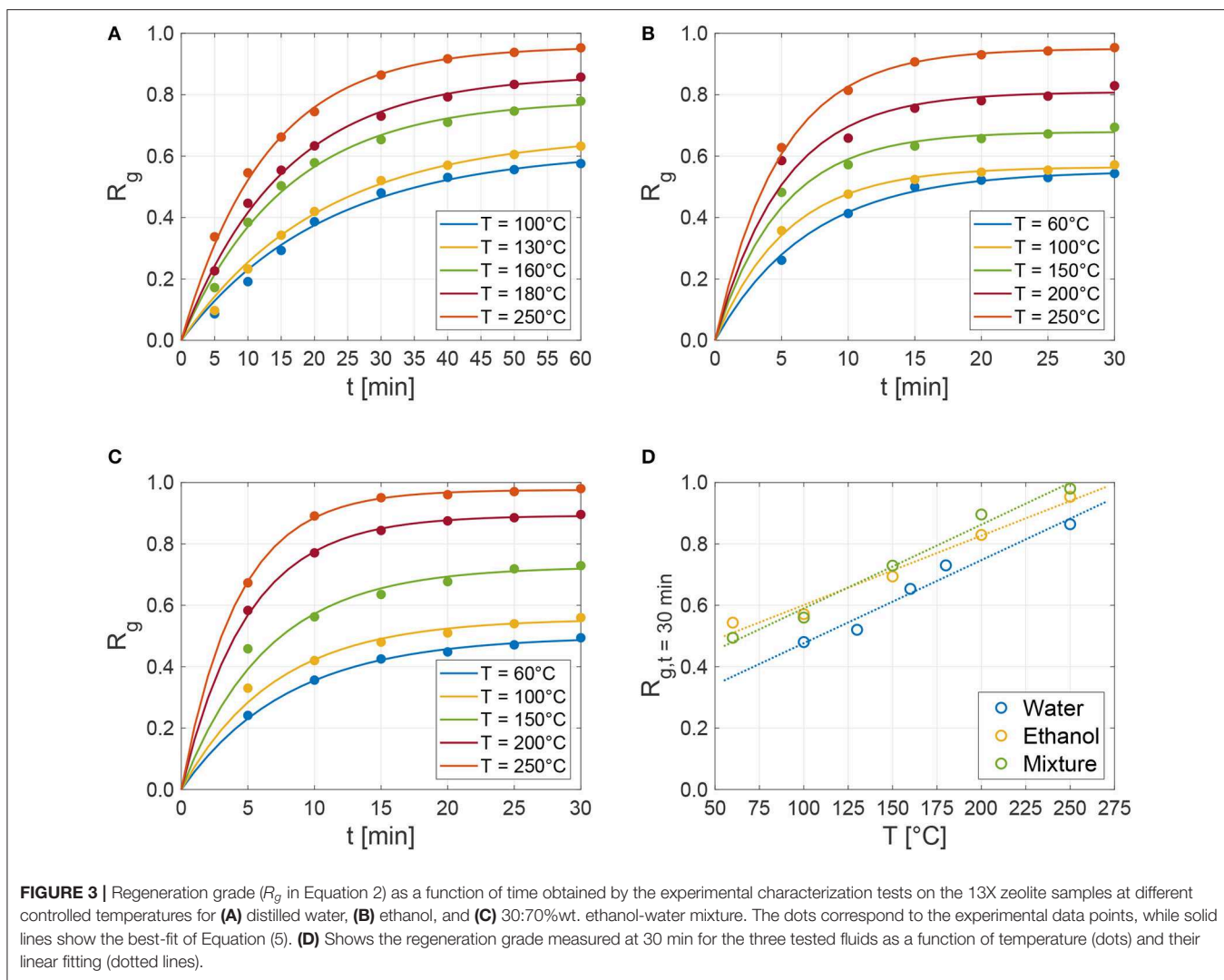
Twelve repetitions have been performed, using a new sample of zeolite for each test. The average quantity of loaded liquid over the twelve repetitions is $\phi = 0.50 \pm 0.02$ for water, $\phi = 0.40 \pm 0.02$ for ethanol, and $\phi = 0.48 \pm 0.04$ for their mixture, where quantities are reported in terms of mean ± 2 standard deviation.

These results show that water has the highest load in the zeolite and ethanol the lowest one, while intermediate values are found for the mixture. In fact, the amount of loaded sorbate depends on the affinity between its fluid molecules and the zeolite surface, and on the size of the fluid molecules with respect to that of the pores and cages in the zeolite framework. Ethanol and water are both polar liquids; yet, the kinetic diameter of water molecules is about 2.96 \AA , while ethanol ones about 4.30 \AA (La Rocca et al., 2019). Zeolite 13X has average pore size around 9 \AA , which allows intrusion of both molecules; however, also because of their smaller size, water molecules can achieve larger adsorption on the zeolite structure.

Note that, while little is known for ethanol and relative mixtures in the literature, several works previously tested water vapor sorption on 13X zeolite (Mette et al., 2014b; Frazzica and Freni, 2017; Pinheiro et al., 2018). The latter investigations report $\phi \approx 0.34$ for the water vapor adsorption on 13X zeolite at $T = 20^\circ\text{C}$ and saturation conditions, namely $p = 0.0234$ bar. Therefore, the larger water loading measured in our experiments could be ascribed to the higher testing pressure, which is more than 40 times larger than the saturation one and may cause additional liquid infiltration into the zeolite pores, and to the possible presence of residual liquid water on the surface of the zeolite bead (see section 3.3 for a discussion on this).

3.2. Dehydration Process

The experimental regeneration grade as a function of time obtained on the fully hydrated zeolite samples is reported in



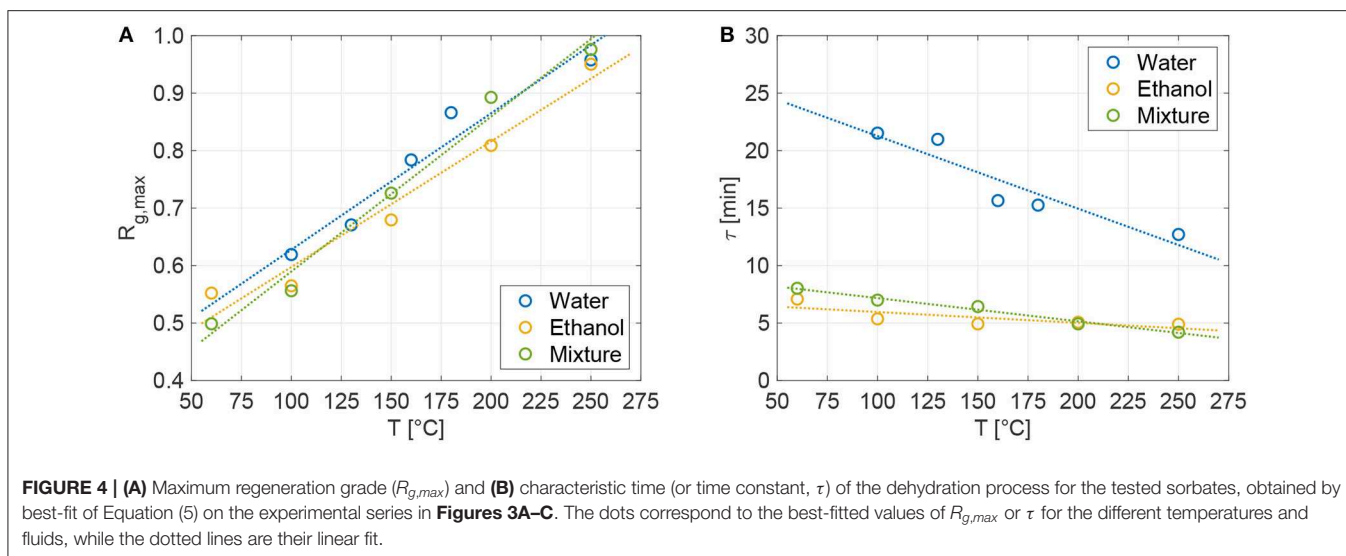
Figures 3A–C (dots) for the three tested fluids. The dehydration temperature has been made vary in a large range of values, to assess the release dynamics of the different sorption pairs. At a given temperature, water presents a slower liquid release than ethanol and mixture, which have instead similar characteristic regeneration times. This can be appreciated in **Figure 3D**, where the regeneration grade measured after 30 min at different temperatures is reported. At 100°C, for example, the amount of water released from the zeolite is about 45% respect to fully hydrated conditions, while this quantity is close to 60% for the ethanol and mixture sorbates. This different release rate could be attributed to the different affinity of the fluid molecules with the surface of the zeolite pores. This is demonstrated by the fact that water molecules are smaller in size than ethanol molecules—mean diameter around 2.96 and 4.30 Å respectively—which should ease their mobility within the zeolite framework (mean pore size equal to 9 Å); yet, water shows a slower release rate, which is due to the higher affinity of water molecules with the surface of the zeolite. **Figures 3A,B** allow to appreciate this effect for the two pure fluids (water and ethanol), while **Figure 3C**

shows the intermediate behavior of the mixture. As the figures show, temperature has a strong effect on the regeneration grade, which, for e.g., water, increases from around 60% at 100°C to 90% at 250°C after 60 min. A similar behavior is observed for ethanol and mixture (see also trends after 30 min in **Figure 3D**).

For all the tested sorbates and temperatures, the experimental data on the regeneration grade show a clear trend as a function of time, which can be accurately recovered—at least for the considered duration of experiments—by the following exponential expression

$$R_g = R_{g,max} (1 - e^{-t/\tau}), \tag{5}$$

with $R_{g,max}$ being the maximum regeneration grade and τ the characteristic regeneration time per each sorbent-sorbate pair and temperature. The characteristic regeneration time is the time constant of the exponential-decay term in the above equation, and represents the time at which the regeneration grade is around 63% its maximum value. All the obtained



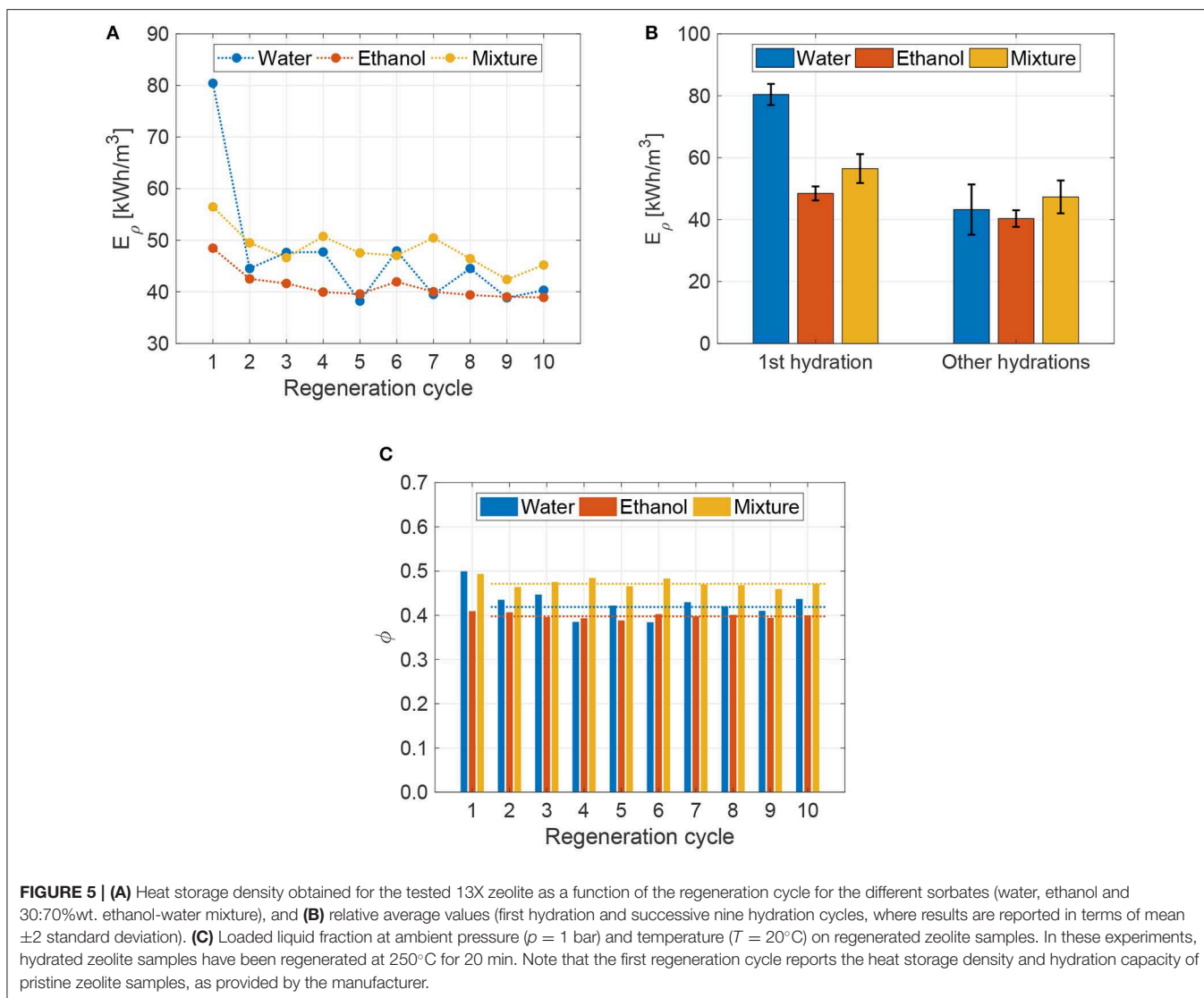
experimental series (dots in **Figures 3A–C**) have been best-fitted with the proposed exponential form in Equation (5), obtaining the maximum regeneration grade and characteristic time (constant) per each tested temperature. The resulting functions are shown in **Figure 3A** (water, $R^2 \geq 0.98$), **Figure 3B** (ethanol, $R^2 \geq 0.85$), and **Figure 3C** (mixture, $R^2 \geq 0.92$) using solid lines. **Figure 4A** shows that the best-fitted $R_{g,max}$ are linearly dependent on temperature; whereas, no significant differences are observed between the three tested fluids. Instead, **Figure 4B** shows that water has slower characteristic regeneration times τ with respect to the other tested sorbates. This implies that ethanol and mixture completely regenerate in around 30 min, while water still regenerates after 60 min and, according to the results of the fitting, would require longer times to eventually achieve the maximum possible regeneration at a given temperature. Indeed, while the characteristic release times of ethanol and mixture slightly change with temperature, the water release time is remarkably more sensitive to temperatures.

3.3. Heat Storage Density

The heat storage density of the considered working pairs has been first measured on new samples of zeolite, which, therefore, did not experience any hydration/dehydration cycles before. Results in **Figures 5A,B** show that water hydration provides higher heat storage density (80 kWh/m^3) with respect to ethanol (49 kWh/m^3) and mixture (56 kWh/m^3) ones. Such behavior originates from the better affinity between water molecules and zeolite 13X, as confirmed by the hydration tests in **Figure 2**. Coherently, the 30:70wt. ethanol-water mixture shows a 15% enhancement in heat storage density with respect to the pure ethanol sorbate. Note that the heat storage density of water vapor on 13XBFK zeolite shown in previous works (Mette et al., 2014; Lehmann et al., 2017) is 2–3 times higher with respect to the values measured here. The suboptimal performance observed in our tests are due to the implemented hydration process, which employs part of the released heat of adsorption to drive the phase change of the sorbate from liquid to vapor. In fact,

the ideal performance of water vapor adsorption on 13XBFK zeolite are (Mette et al., 2014b; Pinheiro et al., 2018): heat of adsorption approximately equal to $\Delta h_{ads} = 3,500 \text{ kJ/kg}$ (released energy per kilogram of adsorbed water, that is 63 kJ/mol); maximum water vapor load on zeolite $\phi = 0.34$. Therefore, considering $\rho_{zeo} = 800 \text{ kg/m}^3$, the ideal heat storage density of the water-13XBFK pair would be equal to $E_{\rho}^{id} = 265 \text{ kWh/m}^3$ in case of purely vapor hydration. However, in our case, the liquid water should be vaporized before being able to adsorb on the surface of zeolite pores: considering an enthalpy of vaporization equal to $\Delta h_{vap} = 2,454 \text{ kJ/kg}$ ($T = 20^\circ\text{C}$) and $\phi = 0.34$, the residual thermal energy available from the adsorption process is estimated to be $E_{\rho} = 79 \text{ kWh/m}^3$, in good agreement with our measures on new samples. This calculation also proves that the higher water load observed in our experiments ($\phi = 0.50$) could be explained by a residual quantity of liquid water on the surface of the zeolite bead after the hydration process, which is not involved in the adsorption process. Clearly, the liquid hydration is inefficient with respect to the typical vapor one; however, it does not require vacuum reactors and cumbersome auxiliary systems therefore allowing a simpler assembly.

The heat storage density has been also evaluated for zeolite samples regenerated up to 10 times, to assess the cyclability of the hydration/dehydration process. Among the different regeneration options in terms of temperature and time, we decided—for illustrative purposes—to regenerate the zeolite for 20 min at 250°C . Note that the considered dehydration temperature is kept far from the autoignition temperature of ethanol, that is 425°C (Dimian et al., 2014). The obtained heat storage densities per each regeneration cycle are reported in **Figure 5A**; whereas, **Figure 5B** shows their values averaged over the 9 regeneration cycles following the first hydration. Experiments show that the heat storage density of the first hydration is significantly higher than the ones from regenerated zeolite samples. This reduction in heat storage density is associated with the residual sorbate



in the zeolite after regeneration, which limits its successive hydration capability (see **Figure 5C**) and is clearly dependent on the considered regeneration protocol. However, after this initial drop in heat storage performance, E_ρ presents only slight decreases in the successive hydration/dehydration cycles, in average: -0.81 kWh/m³ per cycle for the water sorbate; -0.38 kWh/m³ per cycle for the ethanol; -0.59 kWh/m³ per cycle for the mixture. Since water sorbate requires higher regeneration temperatures (see **Figure 3D**) and has slower dehydration kinetics (see **Figure 4B**) than ethanol and mixture ones, the zeolite samples regenerated from water show more pronounced degradation of heat storage density with successive cycles (see **Figure 5B**) (Kohler and Müller, 2017). This progressive reduction in the heat storage density denotes a degradation of the zeolite sorbent, which has been associated by previous works with a minor structure decomposition and formation of amorphous non-porous portions in the sorbent material (Ristić et al., 2018).

Furthermore, the handling of zeolite samples during the successive tests may eventually lead to the generation of diffusion resistances (surface barriers) related to surface pore blockage or narrowing, which may hinder the sorbate intrusion into the zeolite framework (Heinke et al., 2014; Fasano et al., 2016b).

Figure 5C reports the fraction of loaded sorbate with respect to the sorbent mass for 10 successive hydration/dehydration cycles. These results confirm that the employed dehydration process (20 min at 250°C) is suitable to (almost) fully regenerate the zeolite from ethanol and mixture; whereas, a substantial amount of water remains in the zeolite pores after the regeneration. In detail, the mean hydration of regenerated zeolites is: $\phi = 0.42 \pm 0.04$ for water, $\phi = 0.40 \pm 0.01$ for ethanol, and $\phi = 0.47 \pm 0.02$ for the mixture, where quantities are reported in terms of mean ± 2 standard deviation. By comparing these results with the ones in **Figure 2**, ethanol shows no performance degradation in terms of hydration capacity with

respect to the new samples of zeolite, while water presents a 16% reduction in the hydration capability. Remarkably, the mixture maintains similar hydration performance to that of the new samples of zeolite (only 2% reduction).

4. DISCUSSION

The results from the previous thermal characterization show that the 30:70wt. ethanol-water mixture represents a good compromise between high heat storage density for several hydration/dehydration cycles, low regeneration times and temperatures, and low freezing point with respect to that of the pure water and ethanol sorbates. In this section, we provide an illustrative example application of the proposed thermal energy storage system in practice. To this, we consider a portable electric power generator operating in cold climates, and envision the improvement of the efficiency of its Diesel engine during the cold-start using waste heat recovered from the exhaust gases and stored using the proposed TES system. These Diesel generators are typically employed in remote areas for electricity production, in case of e.g., interruptions of the electric service (Morciano et al., 2019). Given their auxiliary scope, these generators are not typically subject to frequent start-stop cycling, which makes them lend to a TES system able to store thermal energy for long periods with negligible losses. This is the case of the proposed solution that, relying on a simplified thermo-chemical heat storage approach, has the pivotal advantage of long-term heat storage over technologies based on sensible/latent heat. In very cold climates indeed, low temperatures may lead to several issues, such as a large concentration of CO and C_nH_n in the exhausts, reduced engine resource time, high load on starter and accumulator and increased fuel consumption during the cold-start (Diemand, 1992), due to the high viscosity of fuel and lubricant and to the difficult ignition at low temperatures (Piperel et al., 2013). On the one side, the use of Winter or Arctic Diesels can prevent the risk of fuel gelling and filter clogging in cold weather conditions (Mitchell and Chandler, 1998); on the other side, cylinders are typically pre-heated by means of glowplugs (Lindl and Schmitz, 1999). The pre-heating of fuel, engine lubricant and/or coolant further improves the engine starting process in terms of reliability and efficiency, while reducing the cold-start extra emissions (Andrews et al., 2007; Roberts et al., 2014). Sensible and latent TES systems recovering the thermal energy from the exhausts have been demonstrated to improve the cold-start performance of engines (Jarrier et al., 2000; Vasiliev et al., 2000); however, they may not be suitable for emergency power systems where the engine operates just a few hours per year and thus successive heat charge/discharge phases could be far in time.

A TES system based on zeolite sorbent and liquid sorbate, instead, could be an inexpensive and reliable solution to recover the thermal energy from engine exhausts (Kauranen et al., 2010), store it for a long time, and then release it when necessary to pre-heat the emergency power system during the cold-start. In the schematics reported in **Figure 6**, the heat discharge and charge

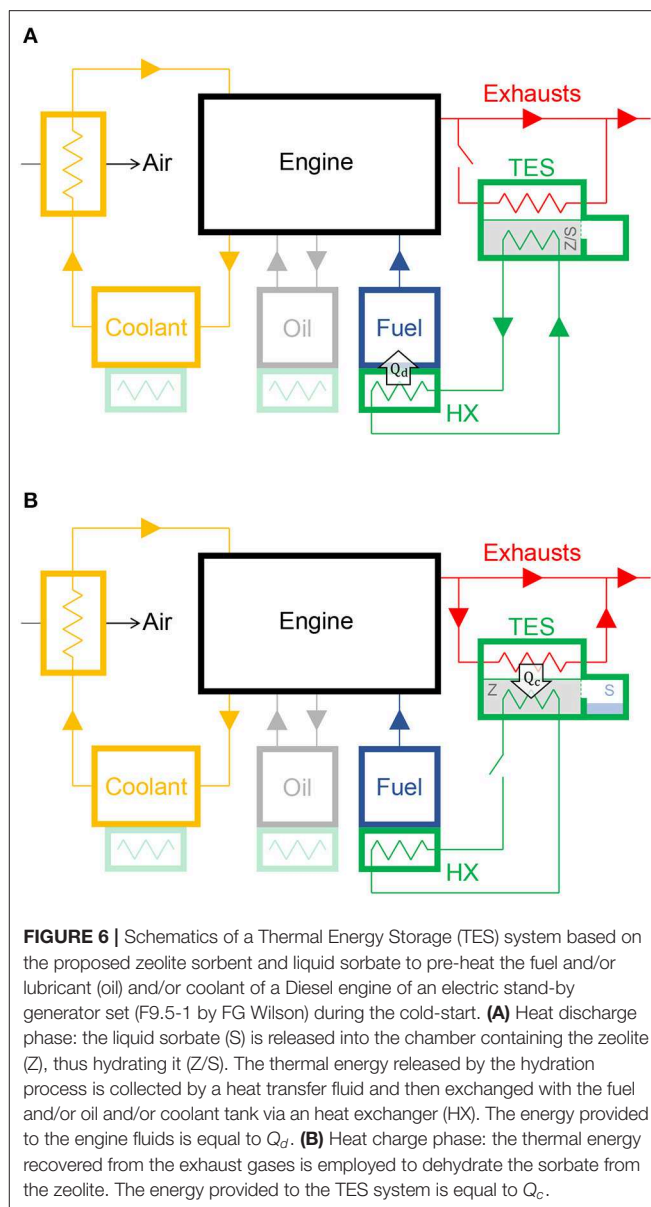


FIGURE 6 | Schematics of a Thermal Energy Storage (TES) system based on the proposed zeolite sorbent and liquid sorbate to pre-heat the fuel and/or lubricant (oil) and/or coolant of a Diesel engine of an electric stand-by generator set (F9.5-1 by FG Wilson) during the cold-start. **(A)** Heat discharge phase: the liquid sorbate (S) is released into the chamber containing the zeolite (Z), thus hydrating it (Z/S). The thermal energy released by the hydration process is collected by a heat transfer fluid and then exchanged with the fuel and/or oil and/or coolant tank via a heat exchanger (HX). The energy provided to the engine fluids is equal to Q_d . **(B)** Heat charge phase: the thermal energy recovered from the exhaust gases is employed to dehydrate the sorbate from the zeolite. The energy provided to the TES system is equal to Q_c .

phases of the TES system are depicted. During the discharge phase (**Figure 6A**), the liquid sorbate hydrates the dry zeolite, the thermal energy released by the hydration process is collected by a heat transfer fluid and then exchanged with the fuel and/or oil and/or coolant tank via an heat exchanger. As a first approximation, the energy provided to the engine fluids during the discharge phase can be estimated as:

$$Q_d = m_f c_{p,f} \Delta T_f = E_p V_{zeo} - Q_{loss}, \quad (6)$$

being Q_{loss} the heat losses in the system, m_f , $c_{p,f}$ and ΔT_f the mass, specific heat capacity and temperature increase of the engine fluid (i.e., coolant, oil or fuel). During the charge phase (**Figure 6B**), instead, the thermal energy recovered from the exhausts is employed to dehydrate the sorbate from the zeolite.

During this phase, the energy that should be provided to the TES system can be computed as:

$$Q_c = \dot{m}_{ex} c_{p,ex} \Delta T_{ex} \Delta t_c = E_{\rho}^{id} V_{zeo} + (k_{liq} - 1) m_{liq} \phi h (c_{p,liq} \Delta T_{liq} + \Delta h_{vap,liq}), \quad (7)$$

where \dot{m}_{ex} , $c_{p,ex}$ and ΔT_{ex} are the mass flow rate, specific heat capacity and temperature decrease of the exhaust gases, while Δt_c is the charge time. Moreover, Equation (7) also presents: E_{ρ}^{id} , that is the ideal thermal energy density of the sorption pair, as from the isosteric heat of adsorption (Fasano et al., 2017); $c_{p,liq}$, ΔT_{liq} and $\Delta h_{vap,liq}$, namely the specific heat capacity, temperature increase and heat of vaporization of the excess liquid sorbate (e.g., ethanol or ethanol-water mixture), if any.

In the followings, a TES system based on the tested 13X zeolite hydrated by ethanol ($E_{\rho} = 49 \text{ kWh/m}^3$; $\phi = 0.40$ after multiple regenerations at 250°C) or the 30:70%wt. ethanol-water mixture ($E_{\rho} = 56 \text{ kWh/m}^3$; $\phi = 0.47$ after multiple regenerations at 250°C) is considered. A zeolite volume of $V_{zeo} = 2 \text{ L}$ is taken for all the analyses, therefore leading to a storable thermal energy equal to 98 Wh (ethanol) or 112 Wh (mixture). Severe cold-start conditions are considered, namely an ambient temperature equal to -20°C , which is anyway above the freezing point of both ethanol and mixture. For the sake of simplicity, heat losses are estimated parametrically as $Q_{loss} = 0.5 E_{\rho} V_{zeo}$ (to be conservative). The analysis is carried out considering the commercial generator set (genset) F9.5-1 by FG Wilson, which has the following characteristics: 10.5 kW Diesel engine; 7.6 kW electric output at 50 Hz; mass flow rate of exhausts equal to $2.4 \text{ m}^3/\text{min}$, with 515°C temperature at the outlet of cylinders; 3.1 L/h fuel consumption; capacity of 60 L fuel (Winter Diesel class F, with cold filter plugging point lower than -20°C); capacity of 11.4 L coolant (50:50 water-glycol mixture, freezing point equal to -35°C); capacity of 4.1 L lubricant (e.g., Mobil Delvac TM Genuine CF-4 Oil 15W-40, pour point equal to -24°C).

In the first application case, a tank containing 3 L of fuel (corresponding to approximately 1 h of genset operations) could be pre-heated by the zeolite during the engine starting. As reported in **Table 1**, this would lead to a potential increase of approximately 40°C in the fuel temperature, which would sharply decrease its kinematic viscosity from $16.82 \text{ mm}^2/\text{s}$ (-20°C) to either $3.46 \text{ mm}^2/\text{s}$ (23.5°C , zeolite hydrated by mixture) or $3.94 \text{ mm}^2/\text{s}$ (18.1°C , zeolite hydrated by ethanol) (Daučík et al., 2008).

In the second application case, the whole tank of the lubricant (4.1 L) could be pre-heated by the TES system during the engine starting. As reported in **Table 1**, this would lead to a potential increase of approximately 30°C in the lubricant temperature, which would reduce its dynamic viscosity from $2,000 \text{ mPa s}$ (-20°C) to either 200 mPa s (11.2°C , mixture) or 300 mPa s (7.3°C , ethanol) (Roberts et al., 2014). Such pre-heating of the lubricant would have a positive impact on the Friction Mean Effective Pressure (FMEP) required to overcome the engine friction during the cold-start, which would be lowered from 6 bar (-20°C) to either 3.5 bar (mixture) or 4 bar (ethanol) (Roberts et al., 2014).

TABLE 1 | Different application cases of a TES system based on 13X zeolite and liquid sorbate (MIX: 30:70%wt. ethanol-water mixture; ETH: ethanol), which is envisioned to increase the temperature of the engine fluids of a genset (F9.5-1 by FG Wilson) during the cold-start.

Quantity	Fuel	Lubricant	Coolant
V_f [L]	3	4.1	11.4
m_f [kg]	2.6	3.6	12.4
$T_{f,e}^{\text{MIX}}$ [$^{\circ}\text{C}$]	23.5	11.2	-15.0
$T_{f,e}^{\text{ETH}}$ [$^{\circ}\text{C}$]	18.1	7.3	-15.6

Starting from an ambient temperature equal to -20°C , the V_f volume (m_f mass) of engine fluid is heated up to $T_{f,e}$ temperature, in case of both mixture and ethanol sorbates.

In the third application case, the whole tank of the coolant (11.4 L) could be pre-heated by the zeolite at the engine starting. As reported in **Table 1**, this would lead to a potential increase of approximately 5°C in the coolant temperature, namely from -20°C to either -15.0°C (mixture) or -15.6°C (ethanol), with a limited change in the viscosity.

Finally, considering for instance $\Delta T_{ex} = 20^{\circ}\text{C}$, $k_{liq} = 1.2$ and $E_{\rho}^{id} \approx 3E_{\rho}$ (similarly to what observed for the water sorbate, to be conservative), the TES system could be fully regenerated after approximately 59 min (mixture) or 46 min (ethanol) of genset operation at steady-state conditions, which seem to be compatible with the typical functioning of engines for emergency power systems.

5. CONCLUSIONS

The experimental characterization of a commercially-available zeolite for sorption heat storage has been carried out and reported. The considered zeolite, 13X type, has been chosen for its suitability to long-term thermal energy storage even after multiple hydration/dehydration cycles. Three different liquid sorbates have been analyzed for the zeolite hydration, namely distilled water, ethanol and a 30:70%wt. ethanol-water mixture. The ethanol and related mixture in water have been chosen for their low freezing point (-114°C and -20°C , respectively), which makes them suitable for utilization in severe low temperatures.

The different sorption pairs have been experimentally characterized in terms of hydration capacity, dehydration dynamics and heat storage density at ambient pressure. Dehydration tests have shown that ethanol and mixture tend to dehydrate faster and at lower temperatures than water, due to the higher affinity of water molecules with the surface of zeolite pores with respect to ethanol. On the other hand, the water-zeolite pair presents the highest heat storage density; therefore, the mixture represents a good compromise between energy storage density and dehydration temperature.

Although the thermal performance of zeolite-liquid hydration is lower than those typically reported for vapor hydration, using liquids may still represent an option when simple design and long-term storage are required. This possibility has been demonstrated through an illustrative example

application, where a compact volume of the proposed sorption materials could improve the performance at cold-start of emergency power systems based on internal combustion engines.

DATA AVAILABILITY STATEMENT

The raw data supporting the conclusions of this manuscript will be made available by the authors, without undue reservation, to any qualified researcher.

AUTHOR CONTRIBUTIONS

PA, EC, and MF contributed conception and design of the study. MF and LB analyzed the data and wrote the manuscript. AL and

MZ performed the experiments and wrote the first draft of the manuscript. All authors contributed to manuscript revision, read, and approved the final version.

FUNDING

The authors acknowledge funding from DENSO Thermal Systems (Technical European Centre, Italy).

ACKNOWLEDGMENTS

The authors acknowledge Antonino Monteleone and Paride Ottaviani for supporting the experimental activity; Marco Rossetto, Cristiano Massano, Matteo Biglia, and Domenico Vitali for technical discussions.

REFERENCES

- Aguiar, P., Miyauchi, E., and Baumgartner, L. (2013). *Thermal Management Solutions to Reduce Fuel Consumption*. Technical report, SAE Technical Paper, Behr Brasil Ltda. doi: 10.4271/2013-36-0246
- Alberghini, M., Morciano, M., Bergamasco, L., Fasano, M., Lavagna, L., Humbert, G., et al. (2019). Coffee-based colloids for direct solar absorption. *Sci. Rep.* 9:4701. doi: 10.1038/s41598-019-39032-5
- Alva, G., Lin, Y., and Fang, G. (2018). An overview of thermal energy storage systems. *Energy* 144, 341–378. doi: 10.1016/j.energy.2017.12.037
- Andreozzi, A., Buonomo, B., Ercole, D., and Manca, O. (2018). Solar energy latent thermal storage by phase change materials (PCMS) in a honeycomb system. *Ther. Sci. Eng. Prog.* 6, 410–420. doi: 10.1016/j.tsep.2018.02.003
- Andreozzi, A., Buonomo, B., Manca, O., Mesolella, P., and Tamburrino, S. (2012). Numerical investigation on sensible thermal energy storage with porous media for high temperature solar systems. *J. Phys.* 395:012150. doi: 10.1088/1742-6596/395/1/012150
- Andrews, G. E., Ounzain, A. M., Li, H., Bell, M., Tate, J., and Ropkins, K. (2007). *The Use of a Water/Lube Oil Heat Exchanger and Enhanced Cooling Water Heating to Increase Water and Lube Oil Heating Rates in Passenger Cars for Reduced Fuel Consumption and CO₂ Emissions During Cold Start*. Technical report, SAE Technical Paper, The University of Leeds. doi: 10.4271/2007-01-2067
- Ap, N., and Golm, N. (1995). “Insulated expansion tank (iet) and thermal storage for engine cold start,” in *1995 SAE International Congress and Exposition*, SAE Technical Paper, 950994. doi: 10.4271/950994
- Baerlocher, C., McCusker, L., and Olson, D. (2007). *Atlas of Zeolite Framework Types, 6th Edn*. Amsterdam: Elsevier.
- Bergamasco, L., Alberghini, M., and Fasano, M. (2019). Nano-metering of solvated biomolecules or nanoparticles from water self-diffusivity in bio-inspired nanopores. *Nanoscale Res. Lett.* 14:336. doi: 10.1186/s11671-019-3178-5
- Bocca, A., Bergamasco, L., Fasano, M., Bottaccioli, L., Chiavazzo, E., Macii, A., et al. (2018). Multiple-regression method for fast estimation of solar irradiation and photovoltaic energy potentials over Europe and Africa. *Energies* 11:3477. doi: 10.3390/en11123477
- Buonomo, B., Ercole, D., Manca, O., and Nardini, S. (2018). Nanoparticles and metal foam in thermal control and storage by phase change materials. *Handb. Ther. Sci. Eng.* 1, 859–883. doi: 10.1007/978-3-319-26695-4_39
- Cabeza, L. F. (ed.). (2015). *Advances in Thermal Energy Storage Systems: Methods and Applications*. Cambridge, UK: Woodhead Publishing.
- Cabeza, L. F., Gutierrez, A., Barreneche, C., Ushak, S., Fernández, G., Fernández, A. I., et al. (2015). Lithium in thermal energy storage: a state-of-the-art review. *Renew. Sustain. Energy Rev.* 42, 1106–1112. doi: 10.1016/j.rser.2014.10.096
- Calabrese, L., Brancato, V., Bonaccorsi, L., Frazzica, A., Capri, A., Freni, A., et al. (2017). Development and characterization of silane-zeolite adsorbent coatings for adsorption heat pump applications. *Appl. Ther. Eng.* 116, 364–371. doi: 10.1016/j.applthermaleng.2017.01.112
- Chidambaram, L., Ramana, A., Kamaraj, G., and Velraj, R. (2011). Review of solar cooling methods and thermal storage options. *Renew. Sustain. Energy Rev.* 15, 3220–3228. doi: 10.1016/j.rser.2011.04.018
- Cot-Gores, J., Castell, A., and Cabeza, L. F. (2012). Thermochemical energy storage and conversion: a state-of-the-art review of the experimental research under practical conditions. *Renew. Sustain. Energy Rev.* 16, 5207–5224. doi: 10.1016/j.rser.2012.04.007
- CWK-BK datasheets (2019). *Chemiewerk Bad Köstritz GmbH, Germany*. Available online at: <http://www.cwk-bk.de/en/>
- Daučík, P., Višňovský, J., Ambro, J., and Hájeková, E. (2008). Temperature dependence of the viscosity of hydrocarbon fractions. *Acta Chimica Slovaca* 1, 43–57.
- Diaz-González, F., Sumper, A., Gomis-Bellmunt, O., and Villafáfila-Robles, R. (2012). A review of energy storage technologies for wind power applications. *Renew. Sustain. Energy Rev.* 16, 2154–2171. doi: 10.1016/j.rser.2012.01.029
- Diemand, D. (1992). Winter operability: equipment problems and their remedies. *J. Cold Regions Eng.* 6, 124–137. doi: 10.1061/(ASCE)0887-381X(1992)6:3(124)
- Dimian, A. C., Bildea, C. S., and Kiss, A. A. (2014). “Health, safety and environment,” in *Computer Aided Chemical Engineering*, Vol. 35, eds A. C. Dimian, C. S. Bildea, and A. A. Kiss (Amsterdam: Elsevier), 649–678. doi: 10.1016/B978-0-444-62700-1.00016-4
- Donkers, P., Pel, L., and Adan, O. (2016). Experimental studies for the cyclability of salt hydrates for thermochemical heat storage. *J. Energy Storage* 5, 25–32. doi: 10.1016/j.est.2015.11.005
- Engel, G., Asenbeck, S., Köll, R., Kerskes, H., Wagner, W., and van Helden, W. (2017). Simulation of a seasonal, solar-driven sorption storage heating system. *J. Energy Storage* 13, 40–47. doi: 10.1016/j.est.2017.06.001
- Farid, M. M., Khudhair, A. M., Razack, S. A. K., and Al-Hallaj, S. (2004). A review on phase change energy storage: materials and applications. *Energy Convers. Manage.* 45, 1597–1615. doi: 10.1016/j.enconman.2003.09.015
- Fasano, M., Borri, D., Cardellini, A., Alberghini, M., Morciano, M., Chiavazzo, E., et al. (2017). Multiscale simulation approach to heat and mass transfer properties of nanostructured materials for sorption heat storage. *Energy Proc.* 126, 509–516. doi: 10.1016/j.egypro.2017.08.229
- Fasano, M., Borri, D., Chiavazzo, E., and Asinari, P. (2016a). Protocols for atomistic modeling of water uptake into zeolite crystals for thermal storage and other applications. *Appl. Ther. Eng.* 101, 762–769. doi: 10.1016/j.applthermaleng.2016.02.015
- Fasano, M., Humplik, T., Bevilacqua, A., Tsapatsis, M., Chiavazzo, E., Wang, E. N., et al. (2016b). Interplay between hydrophilicity and surface barriers on water transport in zeolite membranes. *Nat. Commun.* 7:12762. doi: 10.1038/ncomms12762
- First, E. L., Gounaris, C. E., Wei, J., and Floudas, C. A. (2011). Computational characterization of zeolite porous networks: an automated approach. *Phys. Chem. Chem. Phys.* 13, 17339–17358. doi: 10.1039/c1cp21731c

- Fleming, E., Wen, S., Shi, L., and da Silva, A. K. (2013). Thermodynamic model of a thermal storage air conditioning system with dynamic behavior. *Appl. Energy* 112, 160–169. doi: 10.1016/j.apenergy.2013.05.058
- Flick, E. W. (1998). *Industrial Solvents Handbook*. Westwood, NJ: Elsevier.
- Frazzica, A., and Freni, A. (2017). Adsorbent working pairs for solar thermal energy storage in buildings. *Renew. Energy* 110, 87–94. doi: 10.1016/j.renene.2016.09.047
- Gaeini, M., van Alebeek, R., Scapino, L., Zondag, H., and Rindt, C. (2018). Hot tap water production by a 4 kw sorption segmented reactor in household scale for seasonal heat storage. *J. Energy Storage* 17, 118–128. doi: 10.1016/j.est.2018.02.014
- Gardie, P., and Goetz, V. (1995). *Thermal Energy Storage System by Solid Absorption for Electric Automobile Heating and Air-Conditioning*. Technical report, SAE Technical Paper, Valeo Climate Control; CNRS/IMP.
- Ginley, D., and Parilla, P. (2013). Solar energy: a common-sense vision. *Front. Energy Res.* 1:3. doi: 10.3389/fenrg.2013.00003
- Gritsuk, I., Volkov, V., Gutarevych, Y., Mateichyk, V., and Verbovskiy, V. (2016). *Improving Engine Pre-start and After-start Heating by Using the Combined Heating System*. Technical report, SAE Technical Paper.
- Guo, X., and Goumba, A. P. (2018). Process intensification principles applied to thermal energy storage systems—a brief review. *Front. Energy Res.* 6:17. doi: 10.3389/fenrg.2018.00017
- Heinke, L., Gu, Z., and Wöll, C. (2014). The surface barrier phenomenon at the loading of metal-organic frameworks. *Nat. Commun.* 5:4562. doi: 10.1038/ncomms5562
- Hoogendoorn, C., and Bart, G. (1992). Performance and modelling of latent heat stores. *Solar Energy* 48, 53–58. doi: 10.1016/0038-092X(92)90176-B
- IEA-ETSAP and IRENA (2013). *Thermal Energy Storage*. Technology Brief.
- Jaguemont, J., Omar, N., Van den Bossche, P., and Mierlo, J. (2018). Phase-change materials (pcm) for automotive applications: a review. *Appl. Ther. Eng.* 132, 308–320. doi: 10.1016/j.applthermaleng.2017.12.097
- Jarrier, L., Champoussin, J., Yu, R., and Gentile, D. (2000). *Warm-up of a D.I. Diesel Engine: Experiment and Modeling*. Technical report, SAE Technical Paper.
- Jha, K. K., and Badathala, R. (2015). *Low Temperature Thermal Energy Storage (TES) System for Improving Automotive HVAC Effectiveness*. Technical report, SAE Technical Paper.
- Kauranen, P., Elonen, T., Wikström, L., Heikkinen, J., and Laurikko, J. (2010). Temperature optimisation of a diesel engine using exhaust gas heat recovery and thermal energy storage (diesel engine with thermal energy storage). *Appl. Ther. Eng.* 30, 631–638. doi: 10.1016/j.applthermaleng.2009.11.008
- Kohler, T., and Müller, K. (2017). Influence of different adsorbates on the efficiency of thermochemical energy storage. *Energy Sci. Eng.* 5, 21–29. doi: 10.1002/ese3.148
- La Rocca, T., Carretier, E., Dhaler, D., Louradour, E., Truong, T., and Moulin, P. (2019). Purification of pharmaceutical solvents by pervaporation through hybrid silica membranes. *Membranes* 9:76. doi: 10.3390/membranes9070076
- Lehmann, C., Beckert, S., Gläser, R., Kolditz, O., and Nagel, T. (2017). Assessment of adsorbate density models for numerical simulations of zeolite-based heat storage applications. *Appl. Energy* 185, 1965–1970. doi: 10.1016/j.apenergy.2015.10.126
- Lindl, B., and Schmitz, H.-G. (1999). *Cold Start Equipment for Diesel Direct Injection Engines*. Technical report, SAE Technical Paper, BERU AG.
- Lizana, J., Chacartegui, R., Barrios-Padura, A., and Valverde, J. M. (2017). Advances in thermal energy storage materials and their applications towards zero energy buildings: a critical review. *Appl. Energy* 203, 219–239. doi: 10.1016/j.apenergy.2017.06.008
- McNaught, A. D., and McNaught, A. D. (1997). *Compendium of Chemical Terminology*, Vol. 1669. Oxford: Blackwell Science.
- Mette, B., Kerskes, H., and Drück, H. (2014a). Experimental and numerical investigations of different reactor concepts for thermochemical energy storage. *Energy Proc.* 57, 2380–2389. doi: 10.1016/j.egypro.2014.10.246
- Mette, B., Kerskes, H., Drück, H., and Müller-Steinhagen, H. (2014b). Experimental and numerical investigations on the water vapor adsorption isotherms and kinetics of binderless zeolite 13x. *Int. J. Heat Mass Transf.* 71, 555–561. doi: 10.1016/j.ijheatmasstransfer.2013.12.061
- Miró, L., Gasia, J., and Cabeza, L. F. (2016). Thermal energy storage (TES) for industrial waste heat (IWH) recovery: a review. *Appl. Energy* 179, 284–301. doi: 10.1016/j.apenergy.2016.06.147
- Mitchell, K., and Chandler, J. (1998). *The Use of Flow Improved Diesel Fuel at Extremely Low Temperatures*. Technical report, SAE Technical Paper; Shell Canada Limited; Exxon Chemical Company. doi: 10.4271/982576
- Morciano, M., Fasano, M., Bergamasco, L., Albiero, A., Lo Curzio, M., Asinari, P., et al. (2019). Sustainable freshwater production using passive membrane distillation and waste heat recovery from portable generator sets. *Appl. Energy* 258:114086. doi: 10.1016/j.apenergy.2019.114086
- Narayanan, S., Kim, H., Umans, A., Yang, S., Li, X., Schifres, S. N., et al. (2017). A thermophysical battery for storage-based climate control. *Appl. Energy* 189, 31–43. doi: 10.1016/j.apenergy.2016.12.003
- N'Tsoukpoe, K. E., Liu, H., Pierrès, N. L., and Luo, L. (2009). A review on long-term sorption solar energy storage. *Renew. Sustain. Energy Rev.* 13, 2385–2396. doi: 10.1016/j.rser.2009.05.008
- Ouden, C. (1981). *Thermal Storage of Solar Energy: Proceedings of an International TNO-Symposium Held in Amsterdam, the Netherlands, 5-6 November 1980*. Amsterdam: Springer.
- Pinheiro, J. M., Salústio, S., Valente, A. A., and Silva, C. M. (2018). Adsorption heat pump optimization by experimental design and response surface methodology. *Appl. Ther. Eng.* 138, 849–860. doi: 10.1016/j.applthermaleng.2018.03.091
- Piperel, A., Perrin, H., Walter, B., Crepeau, G., and Starck, L. (2013). Methodology for estimating the performance of fuels during cold start and idle with the adaptation of a gradation system. *Energy Fuels* 27, 1625–1631. doi: 10.1021/ef3016574
- Ristić, A., Fischer, F., Hauer, A., and Logar, N. Z. (2018). Improved performance of binder-free zeolite γ for low-temperature sorption heat storage. *J. Mater. Chem. A* 6, 11521–11530. doi: 10.1039/C8TA00827B
- Roberts, A., Brooks, R., and Shipway, P. (2014). Internal combustion engine cold-start efficiency: a review of the problem, causes and potential solutions. *Energy Convers. Manage.* 82, 327–350. doi: 10.1016/j.enconman.2014.03.002
- Scapino, L., Zondag, H. A., Bael, J. V., Diriken, J., and Rindt, C. C. (2017). Sorption heat storage for long-term low-temperature applications: a review on the advancements at material and prototype scale. *Appl. Energy* 190, 920–948. doi: 10.1016/j.apenergy.2016.12.148
- Schleussner, C.-F., Rogelj, J., Schaeffer, M., Lissner, T., Licker, R., Fischer, E. M., et al. (2016). Science and policy characteristics of the paris agreement temperature goal. *Nat. Clim. Change* 6:827. doi: 10.1038/nclimate3096
- Shere, L., Trivedi, S., Roberts, S., Sciacovelli, A., and Ding, Y. (2018). Synthesis and characterization of thermochemical storage material combining porous zeolite and inorganic salts. *Heat Transf. Eng.* 40, 1176–1181. doi: 10.1080/01457632.2018.1457266
- Shukla, A. K., Dhami, R., Bhargava, A., and Tiwari, S. (2017). *Development and Optimization of PCM Based Technology for Cooling Applications for Improvement of Fuel Efficiency in Commercial Vehicle*. Technical report, SAE Technical Paper. doi: 10.4271/2017-01-0150
- Stritih, U., and Bombač, A. (2014). Description and analysis of adsorption heat storage device. *J. Mech. Eng.* 60, 619–628. doi: 10.5545/sv-jme.2014.1814
- Vasiliev, L., Burak, V., Kulakov, A., Mishkinis, D., and Bohan, P. (2000). Latent heat storage modules for preheating internal combustion engines: application to a bus petrol engine. *Appl. Ther. Eng.* 20, 913–923. doi: 10.1016/S1359-4311(99)00061-7
- Vasiliev, L. L., Burak, V. S., Kulakov, A. G., Mishkinis, D. A., and Bohan, P. V. (1999). Heat storage device for pre-heating internal combustion engines at start-up. *Int. J. Ther. Sci.* 38, 98–104. doi: 10.1016/S0035-3159(99)80020-8
- Vasta, S., Brancato, V., La Rosa, D., Palomba, V., Restuccia, G., Sapienza, A., et al. (2018). Adsorption heat storage: state-of-the-art and future perspectives. *Nanomaterials* 8:522. doi: 10.3390/nano8070522
- Wang, M., Craig, T., Wolfe, E., LaClair, T. J., Gao, Z., Levin, M., et al. (2017). *Integration and Validation of a Thermal Energy Storage System for Electric Vehicle Cabin Heating*. Technical report, SAE Technical Paper, Mahle Behr Troy Inc.; Oak Ridge National Laboratory; Ford Motor Company. doi: 10.4271/2017-01-0183

- Xue, J., Walnum, H. J., Aall, C., and Næss, P. (2016). Two contrasting scenarios for a zero-emission future in a high-consumption society. *Sustainability* 9:20. doi: 10.3390/su9010020
- Yu, N., Wang, R., and Wang, L. (2013). Sorption thermal storage for solar energy. *Prog. Energy Combust. Sci.* 39, 489–514. doi: 10.1016/j.pecs.2013.05.004
- Zettl, B., Englmaier, G., and Steinmaurer, G. (2014). Development of a revolving drum reactor for open-sorption heat storage processes. *Appl. Ther. Eng.* 70, 42–49. doi: 10.1016/j.applthermaleng.2014.04.069
- Zhang, H., Baeyens, J., Caceres, G., Degreve, J., and Lv, Y. (2016). Thermal energy storage: recent developments and practical aspects. *Prog. Energy Combust. Sci.* 53, 1–40. doi: 10.1016/j.pecs.2015.10.003
- Zhao, R., Liu, J., and Gu, J. (2017). “The effects of cooling structure and li-ion battery specification on the cooling performance of a passive thermal management system,” in *Sensing, Diagnostics, Prognostics, and Control (SDPC), 2017 International Conference on (IEEE)*, 662–669. doi: 10.1109/SDPC.2017.131
- Conflict of Interest:** The authors declare that the research was conducted in the absence of any commercial or financial relationships that could be construed as a potential conflict of interest.
- Copyright © 2019 Fasano, Bergamasco, Lombardo, Zanini, Chiavazzo and Asinari. This is an open-access article distributed under the terms of the Creative Commons Attribution License (CC BY). The use, distribution or reproduction in other forums is permitted, provided the original author(s) and the copyright owner(s) are credited and that the original publication in this journal is cited, in accordance with accepted academic practice. No use, distribution or reproduction is permitted which does not comply with these terms.

NOMENCLATURE

ϕ	Sorbent load [kg/kg]	ρ	Density [kg/m ³]
R_g	Regeneration grade [-]	T	Temperature [°C]
E_ρ	Energy density [kWh/m ³]	Δh_{ads}	Heat of adsorption [J/kg]
m	Mass [kg]	\dot{m}	Mass-flow rate [kg/s]
τ	Time constant [min]	p	Pressure [bar]
Q	Thermal energy [J]	k_{liq}	Excess liquid factor [-]
V	Volume [m ³]	c_p	Specific heat capacity [J/(kg °C)]
Δt	Time interval [s]	Δh_{vap}	Heat of vaporization [J/kg]